Journal of Quantitative Spectroscopy & Radiative Transfer 205 (2018) 91–95

Contents lists available at ScienceDirect

Journal of Quantitative Spectroscopy & Radiative Transfer

journal homepage: www.elsevier.com/locate/jqsrt

Absolute frequencies of water lines near 790 nm with 10^{-11} accuracy

J. Chen[a], T.-P. Hua[a], L.-G. Tao[a], Y.R. Sun[a,b], A.-W. Liu[a,b], S.-M. Hu[a,b,*]

[a] Hefei National Laboratory for Physical Sciences at Microscale, iChem Center, University of Science and Technology of China, Hefei, 230026 China
[b] CAS Center for Excellence and Synergetic Innovation Center in Quantum Information and Quantum Physics, University of Science and Technology of China, Hefei, 230026 China

ARTICLE INFO

Article history:
Received 14 September 2017
Revised 7 October 2017
Accepted 9 October 2017
Available online 12 October 2017

ABSTRACT

Water lines in the infrared are convenient frequency references. We present absolute positions of several $H_2{}^{16}O$ ro-vibrational transitions around 790 nm using comb-locked cavity ring-down saturation spectroscopy. Lamb dips of 6 water lines with saturation power in the range of 70–130 kW/cm^2 were observed and the line positions were determined with an accuracy of 25 kHz, corresponding to a fractional uncertainty of 6.6×10^{-11}. The present work demonstrates the capability to considerably improve the accuracy of the water line positions in the infrared.

© 2017 Elsevier Ltd. All rights reserved.

Ro-vibrational spectroscopy of water vapor is of great interest for its importance in chemical, atmospheric and astronomical studies. Water molecule has an enormous amount of transitions in the infrared region. Because of the ubiquity of water, its absorption lines are the most widely used frequency references in many studies. Spectroscopic databases such as HITRAN [1], GEISA [2], and HITEMP [3] have included a huge amount of water transitions which are mostly from Doppler-broadened spectroscopy, and the accuracy of the line positions is usually limited to 10^{-3}–10^{-4} cm^{-1}. Saturated absorption spectroscopy is the most commonly used method to obtain precise line positions. Golubiatnikov et al. observed Lamb dips of $H_2{}^{16}O$ lines in the region of 0.18–0.56 THz and obtained line positions with a precision of 1 kHz or a fractional uncertainty of 2×10^{-9} [4]. Cazzoli et al. presented hyperfine structures in the rotational spectrum of water from Lamb-dip measurements in the range of 0.3–0.65 THz, and the uncertainty was 0.5 kHz corresponding to a relative accuracy of 8×10^{-10} [5]. Lisak and Hodges presented Lamb dips of a few water lines near 1.40 µm with sub-MHz resolution but without absolute frequencies [6,7]. Using an optical frequency comb, Gambetta et al. presented absolute frequencies with an uncertainty of about 30 kHz for several $H_2{}^{17}O$ and $H_2{}^{18}O$ lines in the region of 1.38 to 1.41 µm, corresponding to a relative accuracy of 1.4×10^{-10} [8].

Here we report the saturated absorption spectroscopy of several $H_2{}^{16}O$ lines near 790 nm. Water lines in this region have been extensively studied by Fourier-transform spectroscopy (FTS) [9–12], intra-cavity laser absorption spectroscopy (ICLAS) [13–15]. The very sensitive cavity ring-down spectroscopy (CRDS) has allowed to record the Doppler-broadened absorption spectrum with an improved signal-to-noise ratio [16]. By using CRDS calibrated by a Fabry–Pérot interferometer made of ultralow-expansion glass (ULE-FPI), our group has reported 73 water lines around 790 nm with a stated uncertainty of 3×10^{-5} cm^{-1}, which is about 0.1% of the line width [17]. The study has been extended to the region of 782–840 nm, and the line positions were reported with an uncertainty of 1.7×10^{-4} cm^{-1} [18]. However, there is no much improvement in the accuracy while using Doppler-broadened spectrum, because it is very difficult to assess the contribution from the line profile model at a precision of 0.1% of the line width. Using comb-locked CRDS to measure Lamb-dip saturation absorption lines of CO at 1566 nm, we demonstrated a possibility to determine the line positions with an uncertainty of 0.5 kHz (relatively 2.6×10^{-12}) [19,20]. Here, we extend the spectral region to 790 nm and present saturation spectroscopy of water lines in this region. Although these lines are relatively weak (line intensities $\sim 2 \times 10^{-24}$ cm/molecule) and the saturation power is considerably high (~100 kW/cm^2), Lamb dips were observed using a diode laser of tens of milliwatts and the line positions were determined with an uncertainty of 25 kHz (relatively 6.6×10^{-11}). The present work demonstrates the potential to significantly improve the accuracy of the water line positions in the infrared.

The main structure of the experimental setup (Fig. 1) includes two locking loops. One locks an external cavity diode laser (ECDL, Toptica DL100) to a temperature-stabilized ring-down (RD) cavity using the Pound-Drever-Hall (PDH) method. The other one locks the RD cavity length by a phase-lock circuit based on the beat frequency between the probe laser and an optical frequency comb. The resonance RD cavity is composed of two high-reflective (HR) mirrors setting apart with a distance of 45.9 cm, corresponding to a free-spectral range of 327 MHz. Each HR mirror has a reflectivity

---

[*] Corresponding author.
E-mail address: smhu@ustc.edu.cn (S.-M. Hu).

https://doi.org/10.1016/j.jqsrt.2017.10.009
0022-4073/© 2017 Elsevier Ltd. All rights reserved.

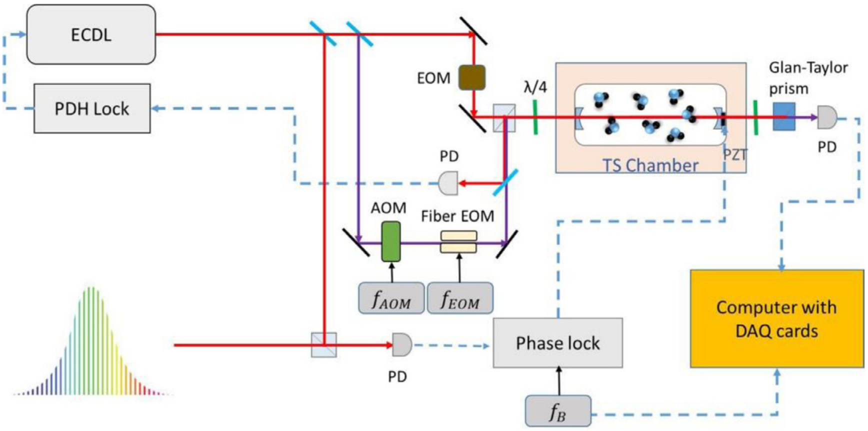

Fig. 1. Configuration of the experimental setup. One beam (red) from ECDL (external cavity diode laser) is used to lock the laser with the cavity; another beam (purple) with a frequency shift of $f_{AOM}+f_{EOM}$ is used for ring-down detecting. The cavity length is locked through the beat signal between ECDL and an optical frequency comb. Abbreviations: AOM: acousto-optical modulator; DAQ: data acquisition system; EOM: electro-optical modulator; PD: photodiode detector; PZT: piezo actuator. (For interpretation of the references to color in this figure legend, the reader is referred to the web version of this article.)

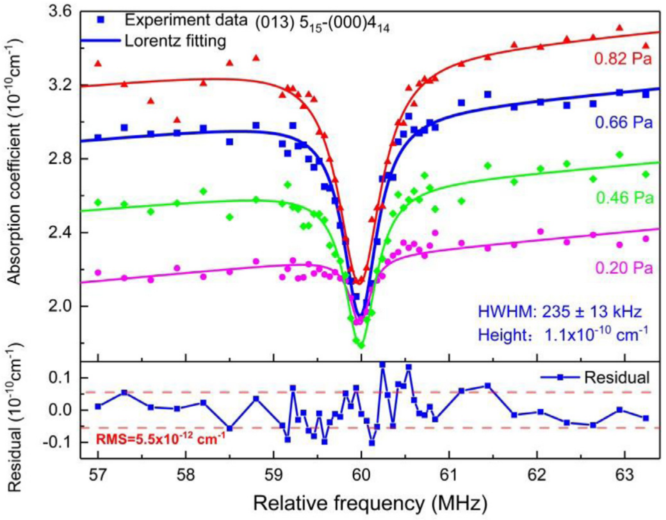

Fig. 2. Lamb-dip spectra of the (013)5_{15}-(000)4_{14} line of $H_2{}^{16}O$ at 12,651.93 cm^{-1}. Spectra were shifted for better illustration. The fitting residuals of the spectrum recorded at 0.66 Pa are given in the lower panel and the root-mean-square (RMS) is 5.5×10^{-12} cm^{-1}.

of 99.995% at 760–820 nm. Therefore, the RD cavity has a finesse of about 7.1×10^4 and a mode width of about 4.6 kHz. The PDH locking servo allows us to lock the probe laser frequency within about 1% of the cavity mode width. The RD cavity is made of aluminum, located in a stainless-steel vacuum chamber. An aluminum shield is used for thermal isolation between the RD cavity and the outer chamber. A feedback circuit controls the heating-current in a wire surrounding the aluminum shield to stabilize its temperature at 300 K. Two platinum thermal sensors are attached at two sides of the RD cavity, which show that the temperature fluctuation is within 2 mK for hours [21].

An optical frequency comb operated at 780 nm is used as the absolute frequency reference. The comb is synthesized by an Er: fiber oscillator (1557 nm) with its repetition frequency (f_r) and carrier offset frequency (f_0) referenced to a GPS-disciplined rubidium clock (SRS FS725). The beat signal between the locking beam and the frequency comb is phase-locked to a radio frequency (f_B), and the digital feedback servo drives a piezo actuator attached on one HR mirror to adjust the length of the RD cavity. When the phase-lock loop is turned on, the RD cavity length is stabilized. As a result, the probe laser frequency, which is locked to a longitudinal mode of the RD cavity, is eventually locked with the frequency comb.

A beam from the probe laser, with its frequency shifted by an acousto-optical modulator (AOM) and an electro-optical modulator (EOM), is used for cavity ring-down spectroscopy. When the overall frequency shift is equal to an integer number times of the free-spectral-range (FSR) of the cavity, a portion of the beam is also coupled into the cavity. The input power of fiber EOM is about 6 mW, leading to the 1st-order sideband power of about 1.1 mW which is coupled into the RD cavity. The RD-probing beam emitted from the cavity is detected by a photodiode (PD) while the laser-locking beam is deflected by a Glan-Tyler prism. When the signal reaches a steady level, a trigger signal is produced to switch off the AOM, which blocks the probe beam and initiates a ring-down event. The ring-down signal is digitized and recorded by a fast digitizer installed in a personal computer. A fitting program based on the Levenberg-Marquardt algorithm is applied to fit the curve to an exponential decay function. The decay time τ is used to determine the absorption coefficient α of the sample in the RD cavity according to the equation,

$$\alpha = \frac{1}{c\tau} - \frac{1}{c\tau_0}, \qquad (1)$$

where c is the speed of light, and τ_0 is the decay time of an empty cavity. Note that during the RD-recording period which lasts typically a few hundred microseconds, the probe laser is kept locking with the RD cavity. When the RD-recording period finishes, the AOM is switched on again, and the light field in the cavity is rebuilt to prepare another RD event. In this way, the spectrum is recorded with a laser locked with sub-kHz precision. The spectral scan is accomplished by tuning the reference frequency f_B of the phase-lock loop,

$$\nu = f_0 + nf_r + f_{AOM} + f_{EOM} + f_B, \qquad (2)$$

where f_{AOM} and f_{EOM} are the radio frequencies driving the AOM and EOM, f_0 and f_r are the carrier offset frequency and repetition frequency of the comb, respectively.

Vapor from deionized water was used in the experiments. The sample pressure was measured by a manometer with a stated uncertainty of 0.5%. As given in the HITRAN database [1], the 5_{15}-4_{14} line in the (013-000) band is located at 12,651.93 cm^{-1}, with an intensity of 2.68×10^{-24} cm/molecule and an Einstein coefficient of 5.1×10^{-3} s^{-1}. In Fig. 2, Lamb dip of the (013)5_{15}-(000)4_{14} line has

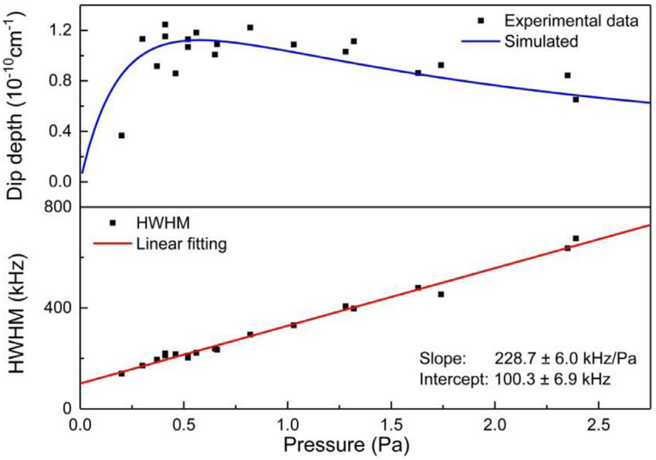

Fig. 3. Depth (upper panel) and width (HWHM, lower panel) of the lamb dip of the $(013)5_{15}$-$(000)4_{14}$ line observed at different sample pressures.

a line width (half width at half maximum, HWHM) of 235 kHz at a sample pressure of 0.66 Pa. The scan step was 300 kHz on the baseline and 60 kHz around the line center. There were 45 data points in one scan which took about 1 min. The spectrum shown in Fig. 2, an average of 104 scans, was fitted by a Lorentzian profile and the fitting residuals were at the level of 1×10^{-11} cm^{-1}, leading to a signal-to-noise ratio of 10. The dip depth is related to the laser power inside the cavity and the sample pressure. In our experiment, the beam waist in the cavity is about 0.5 mm, and the input power is about 1.1 mW which is limited by the EOM. With an enhancement factor of 1.3×10^4, the intra-cavity laser power reaches about 14 W [22], which is about 2.6% of the saturation power.

Fig. 3 shows the depth and width (HWHM) of the Lamb dip of the $(013)5_{15}$-$(000)4_{14}$ line observed at different pressures. The calculated [22,23] depths are also given in the upper panel of the figure, which agrees reasonably with the experimental results. The width of the Lamb dip follows a linear dependence on the sample pressure. A linear fit gives a self-pressure broadening coefficient of 229 kHz/Pa, larger than that of 122 kHz/Pa (0.412 cm^{-1}/atm) given in the HITRAN data base [1]. The width at the zero-pressure limit is 100 kHz, which should be mainly due to the transit-time broadening. At 300 K, the root mean square velocity of H_2O is about 645 m/s, corresponding to a transit-time half width of 161 kHz. The discrepancy probably comes from oversimplified line profile model of the saturation spectrum [20] and the limited signal-to-noise ratio in the measurements. According to the depths and widths of the Lamb dips shown in Fig. 3, in order to pursue a better precision, we chose the sample pressure of about 0.5 Pa to determine the line positions.

In order to investigate the possible pressure shift and power shift at present experimental conditions, we carried out a series of measurements. Fig. 4 shows the line positions of the $(013)5_{15}$-$(000)4_{14}$ line obtained at different pressures and different intra-cavity laser powers. Each data point is derived from an average of about 100–200 scans. As shown in Fig. 4(a), we could not observe a clear pressure-dependent line shift within such a low pressure region. A linear fit of the data in the full pressure range gives a self-pressure shift coefficient of 14.1 ± 5.2 kHz/Pa, quite different from the value −5 kHz/Pa (−0.017 cm^{-1}/atm) given in HITRAN [1]. For this reason, we use a simple average of the positions obtained at sample pressures in the range of 0.2–0.8 Pa. The position of the $(013)5_{15}$-$(000)4_{14}$ line was determined to be 379 295 381 452.5 kHz, with a statistical uncertainty of 2.6 kHz. Upon that, an uncertainty of 7 kHz was included to take into account possible contribution from the pressure shift. We have also measured the spectra using different input laser powers, and the results are given in Fig. 4(b). No power dependence has been observed within the experimental uncertainty. Therefore, a sample pressure of about 0.5 Pa and an intra-cavity power of 14 W are chosen in the measurements for other lines.

The overall uncertainty budget for $(013)5_{15}$-$(000)4_{14}$ line is given as follows. The statistical uncertainty is 2.6 kHz. Systematic uncertainty consists of several parts. As shown in Fig. 2, we did not see asymmetry in the line profile at current experimental noise level, and we use the quotient of the line width and the signal-to-noise ratio, 235/10 = 23.5 kHz, as an estimation of the uncertainty from the line profile model. The uncertainties from the comb frequency and the locking servo are 0.4 kHz and 0.05 kHz, respectively [20]. The uncertainties in the driving frequencies of the AOM

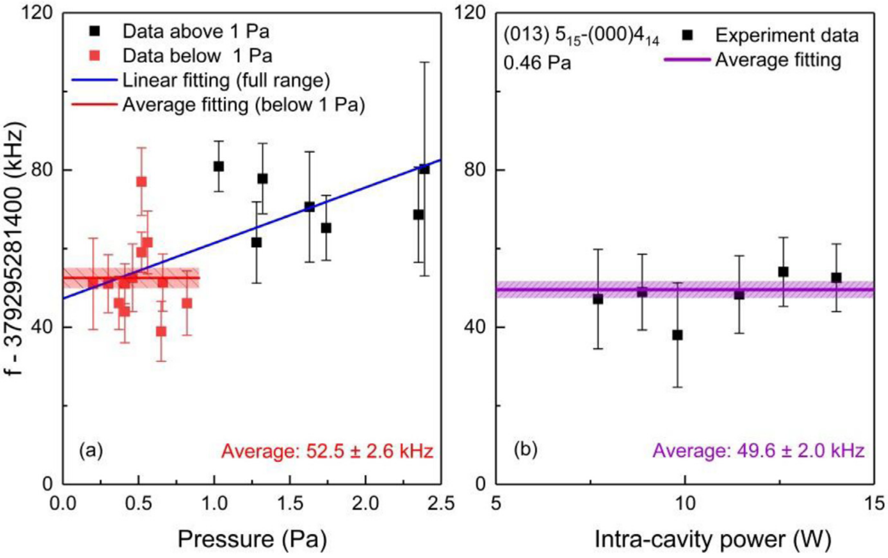

Fig. 4. Position of the $(013)5_{15}$-$(000)4_{14}$ line observed at different sample pressures and different intra-cavity laser powers. Panel (a): weighted average of line position (red) below 1 Pa was about 379 295 281 452.5 ± 2.6 kHz. A linear fit of all the data gives a slope of 14.1 ± 5.2 kHz/Pa and an intercept of 379 295 281 447.3 ± 5.2 kHz. Panel (b): weighted average of the line positions obtained at different intra-cavity laser powers is 379 295 281 449.6 ± 2.0 kHz. (For interpretation of the references to color in this figure legend, the reader is referred to the web version of this article.)

Table 1
Line positions in the 013-000 band and upper level energies obtained in this work (unit: cm^{-1}).

Transition	S[a]	I_S[b]	ν, this work	$\Delta\nu$[c]	E_{lower}[d]	E_{upper}[e])	δ_E[f]
3_{13}–2_{12}	2.98	78.5	12 621.736 436 1(8)	69	79.496 369 9(4)	12 701.232 806 0(9)	781
3_{22}–2_{21}	1.39	128.3	12 629.757 508 8(20)	90	134.901 612 7(4)	12 764.659 121 5(21)	1073
4_{04}–3_{03}	2.97	76.9	12 640.738 200 9(8)	93	136.761 633 0(4)	12 777.499 833 8(9)	663
5_{15}–4_{14}	2.68	67.8	12 651.928 736 5(8)	102	224.838 347 1(6)	12 876.767 083 6(10)	653
4_{13}–3_{12}	2.38	80.3	12 661.108 780 8(8)	109	173.365 777 5(4)	12 834.474 558 3(9)	934
6_{06}–5_{05}	1.94	68.0	12 665.158 348 0(8)	96	325.347 852 6(9)	12 990.506 200 6(12)	842

[a] Line intensity from HITRAN database [1], in 10^{-24} cm/molecule.

[b] Saturation power, calculated according to the formula in Ref. [23], in kW $^{\text{cm-2}}$.

[c] $\Delta\nu = \nu_{Lu} - \nu_{this}$, ν_{Lu} is from work by Lu et al. [17], in 10^{-6} cm^{-1}.

[d] E_{lower} is the lower level energy from Ref. [24].

[e] E_{upper} is the upper level energy calculated from the line position obtained in this work and the lower level energy from Ref. [24].

[f] $\delta E = E_{MARVEL}$-E_{up}, in 10^{-6} cm^{-1}. E_{MARVEL} is the upper level energy from Ref. [25].

and EOM are negligible. The uncertainty due to pressure shift is 7 kHz. The uncertainty due to power shift is estimated to be less than 2 kHz. AC (alternating current) Stark shift is negligible under our experiment conditions. Taking a root mean square velocity of H_2O of about 645 m/s at 300 K, the second-order Doppler shift is -1 kHz. The calculated recoil shift is 18 kHz. Finally, we determined the position of the $(013)5_{15}$–$(000)4_{14}$ line to be 379 295 281 436 $\pm$ 25 kHz with a relative accuracy of 6.6×10^{-11}.

Similar measurements have been carried out for other five lines in the (013-000) band with intensities above 1.3×10^{-24} cm/molecule. Similar accuracy has been obtained for these five lines except the $(013)3_{22}$-$(000)2_{21}$ line for which the saturation power is almost twice as that of the strongest line. We can only get a signal-to-noise ratio of about 3 for the $(013)3_{22}$-$(000)2_{21}$ line, which leads to a relatively larger uncertainty in the position.

Positions of the 6 water lines obtained in this work are presented in Table 1. Their differences from those given in previous Doppler-broadened CRDS measurement [17] are also given in the table. The averaged difference is about 9×10^{-5} cm^{-1}, while the stated uncertainty given in Ref. [17] is about 3×10^{-5} cm^{-1}. A possible reason of the discrepancy could be the long-term drift of the Fabry–Pèrot interferometer made of ultra-low expansion glass (ULE-FPI) used for frequency calibration in previous measurement. Taking the rotational energies of $H_2{}^{16}O$ given in Ref. [24], which have a stated uncertainty of about 0.5×10^{-6} cm^{-1} (15 kHz), we derived the energies of the upper levels. They are also given in Table I. The combined uncertainty is 1–2×10^{-6} cm^{-1}. They are compared with the upper energies E_{MARVEL} which were derived from the analysis of thousands of Doppler-broadened water lines [25]. The stated averaged uncertainty of the upper level energies E_{MARVEL} from [25] is 4.5×10^{-5} cm^{-1}. However, for the 6 upper levels presented in this work, the MARVEL energies have a discrepancy from present data varying between 0.00065 cm$-$1 and 0.00107 cm$-$1.

To summarize, we presented saturation spectroscopy of several $H_2{}^{16}O$ lines around 790 nm using comb-locked cavity ring-down spectroscopy. The absolute frequencies of these lines were determined with an accuracy of 25 kHz (relatively 6.6×10^{-11}), improved by over one order of magnitude. Comparing with the water line frequencies reported in previous Doppler-broadened CRDS study [17], we suggest a shift of -9×10^{-5} cm^{-1} on previous data. Considerably large discrepancy up to 0.001 cm^{-1} has been found in the upper level energies compared with those from the MAVEL analysis. Note that similar measurements can be carried out for an extensive set of molecular lines with moderate line strength ($> 1 \times 10^{-24}$ cm/molecule) in the infrared, and better accuracy is expected for stronger lines. In this way, the accuracy of the molecular frequency references could be considerably improved.

Acknowledgments

This work was jointly supported by NSFC (Nos. 91436209, 21427804, 21688102) and by CAS (No. XDB21020100).

Reference

[1] Gordon IE, Rothman LS, Hill C, Kochanov RV, Tan Y, Bernath PF, et al. The HITRAN2016 molecular spectroscopic database. J Quant Spectrosc Radiat Transf 2017. doi:10.1016/j.jqsrt.2017.06.038.
[2] Jacquinet-Husson N, Armante R, Scott NA, Chedin A, Crepeau L, Boutammine C, et al. The 2015 edition of the GEISA spectroscopic database. J Mol Spectrosc 2016;327:31–72.
[3] Rothman LS, Gordon IE, Barber RJ, Dothe H, Gamache RR, Goldman A, et al. HITEMP, the high-temperature molecular spectroscopic database. J Quant Spectrosc Radiat Transf 2010;111:2139–50.
[4] Golubiatnikov GY, Markov VN, Guarnieri A, Knöchel R. Hyperfine structure of $H_2{}^{16}O$ and $H_2{}^{18}O$ measured by Lamb-dip technique in the 180–560 GHz frequency range. J Mol Spectrosc 2006;240:251–4.
[5] Cazzoli G, Puzzarini C, Harding ME, Gauss J. The hyperfine structure in the rotational spectrum of water: lamb-dip technique and quantum-chemical calculations. Chem Phys Lett 2009;473:21–5.
[6] Lisak D, Hodges JT, Ciurylo R. Comparison of semiclassical line-shape models to rovibrational H_2O spectra measured by frequency-stabilized cavity ring-down spectroscopy. Phys Rev A 2006;73:012507.
[7] Lisak D, Hodges JT. High-resolution cavity ring-down spectroscopy measurements of blended H_2O transitions. Appl Phys B-Lasers Opt 2007;88:317–25.
[8] Gambetta A, Fasci E, Castrillo A, Marangoni M, Galzerano G, Casa G, et al. Frequency metrology in the near-infrared spectrum of $H_2{}^{17}O$ and $H_2{}^{18}O$ molecules: testing a new inversion method for retrieval of energy levels. New J Phys 2010;12:103006.
[9] Toth RA. Measurements of $H_2{}^{16}O$ line positions and strengths: 11 610 to 12 861 cm^{-1}. J Mol Spectrosc 1994;166:176–83.
[10] Flaud JM, Camy-Peyret C, Bykov A, Naumenko O, Petrova T, Scherbakov A, et al. The high-resolution spectrum of water vapor between 11 600 and 12 750 cm^{-1}. J Mol Spectrosc 1997;183:300–9.
[11] Schermaul R, Learner RCM, Newnham DA, Williams RG, Ballard J, Zobov NF, et al. The water vapor spectrum in the region 8600–15 000 cm^{-1}: experimental and theoretical studies for a new spectral line database. J Mol Spectrosc 2001;208:32–42.
[12] Mérienne M-F, Jenouvrier A, Hermans C, Vandaele AC, Carleer M, Clerbaux C, et al. Water vapor line parameters in the 13000–9250cm^{-1} region. J Quant Spectrosc Radiat Transf 2003;82:99–117.
[13] Kalmar B, O'Brien JJ. Quantitative intracavity laser spectroscopy measurements with a Ti:sapphire laser: absorption intensities for water vapor lines in the 790–800 nm region. J Mol Spectrosc 1998;192:386–93.
[14] Mazzotti F, Naumenko OV, Kassi S, Bykov AD, Campargue A. ICLAS of weak transitions of water between 11300 and 12850cm^{-1}: comparison with FTS databases. J Mol Spectrosc 2006;239:174–81.
[15] Campargue A, Mikhailenko S, Liu AW. ICLAS of water in the 770 nm transparency window (12746–13558cm^{-1}). Comparison with current experimental and calculated databases. J Quant Spectrosc Radiat Transf 2008;109:2832–45.
[16] Kassi S, Macko P, Naumenko O, Campargue A. The absorption spectrum of water near 750 nm by CW-CRDS: contribution to the search of water dimer absorption. Phys Chem Chem Phys 2005;7:2460–7.
[17] Lu Y, Li XF, Wang J, Liu AW, Hu SM. H_2O line positions in the 784–795 nm region with 10^{-9} accuracy. J Quant Spectrosc Radiat Transf 2013;118:96–101.
[18] Hu SM, Chen B, Tan Y, Wang J, Cheng CF, Liu AW. Water line positions in the 782–840 nm region. J Quant Spectrosc Radiat Transf 2015;164:37–44.
[19] Wang J, Sun YR, Tao LG, Liu AW, Hua TP, Meng F, et al. Comb-locked cavity ring-down saturation spectroscopy. Rev Sci Instrum 2017;88:043108.

[20] Wang J, Sun YR, Tao L-G, Liu A-W, Hu S-M. Communication: molecular near-infrared transitions determined with sub-kHz accuracy. J Chem Phys 2017;147:091103.

[21] Cheng CF, Wang J, Sun YR, Tan Y, Kang P, Hu SM. Doppler broadening thermometry based on cavity ring-down spectroscopy. Metrologia 2015;52 S385-S93.

[22] Ma LS, Ye J, Dube P, Hall JL. Ultrasensitive frequency-modulation spectroscopy enhanced by a high-finesse optical cavity: theory and application to overtone transitions of C_2H_2 and C_2HD. J Opt Soc Am B 1999;16:2255–68.

[23] Giusfredi G, Bartalini S, Borri S, Cancio P, Galli I, Mazzotti D, et al. Saturated-absorption cavity ring-down spectroscopy. Phys Rev Lett 2010;104:110801.

[24] Furtenbacher T, Császár AG. On employing $H_2{}^{16}O$, $H_2{}^{17}O$, $H_2{}^{18}O$, and $D_2{}^{16}O$ lines as frequency standards in the 15–170 cm^{-1} window. J Quant Spectrosc Radiat Transf 2008;109:1234–51.

[25] Tennyson J, Bernath PF, Brown LR, Campargue A, Császár AG, Daumont L, et al. IUPAC critical evaluation of the rotational–vibrational spectra of water vapor, Part III: energy levels and transition wavenumbers for $H_2{}^{16}O$. J Quant Spectrosc Radiat Transf 2013;117:29–58.